This document is the Accepted Manuscript version of a Published Work that appeared in final form in **Journal of Materials Chemistry C** 10(40) : 15186-15193 (2022), copyright © 2022 The Royal Society of Chemistry. To access the final edited and published work see https://doi.org/10.1039/D2TC03248A

Injectable PEDOT:PSS/cholinium ionic liquid mixed conducting materials for electrocardiogram recordings

Nerea Casado,*[a,f] Sara Zendegi,[a] Liliana C. Tomé,[b] Santiago Velasco-Bosom,[c] Ana Aguzin,[d] Matias Picchio,[d] Miryam Criado-Gonzalez,[a] George G. Malliaras,[c] Maria Forsyth,[a,e,f] and David Mecerreyes[a,f]

Mixed conducting polymer electrodes built from poly(3,4-ethylenedioxythiophene): poly(styrene sulfonate) (PEDOT:PSS) are attracting a great deal of interest in healthcare monitoring. However, the widespread application of this organic conductor in wearable devices is seriously restricted by toxic additives used to enhance its electrical conductivity. Herein, we explored a family of biocompatible ionic liquids (ILs), based on the cholinium cation and different carboxylated anions, as dopants and gelators for PEDOT:PSS to formulate safe bioelectrodes for long-term cutaneous recording. We examined the effect of the IL anion on the ionic-electronic conductivities and physicochemical properties of these soft conductors. Among the different ILs tested, cholinium lactate ([Ch][Lac]) afforded the greatest increase in the materials' electronic conductivity (≈30 S/cm vs. 0.2 S/cm for non-formulated PEDOT:PSS). Moreover, the PEDOT:PSS/IL mixtures formed gels due to supramolecular intereactions. The gels showed a rheological behavior associated to gels with excellent injectability properties. Finally, the performance of PEDOT:PSS/[Ch][Lac] as biocompatible electrodes for electrocardiogram recording is discussed. All in all, the obtained results unveil the effectiveness of cholinum-based ILs as non-toxic dopants of PEDOT:PSS, paving the way to explore novel bioderived electrolytes.

Introduction

Flexible electronics is an exciting research field in seamless expansion, enabling new device applications for energy storage[1,2] and bioelectronics devices,[3] such as motion sensors,[4] stretchable displays,[5] and electrodes for physiological recording[6] and muscle stimulation.[7] In bioelectronics, conducting polymer electrodes based on poly(3,4-ethylenedioxythiophene): poly(styrene sulfonate) (PEDOT:PSS) have shown many advantages in cutaneous recordings, such as a stable conducting state and high signal to noise ratio.[8–10] However, pristine PEDOT:PSS films possess a bulk electrical conductivity of 0.2-0.35 S/cm, which is not satisfactory for many highly demanding applications.[11] This low conductivity is frequently associated with the formation of insulating PSS outer layers encapsulating the conducting PEDOT cores.[12]

Fortunately, the PEDOT:PSS conductivity could be improved by more than 1000-folds through different treatments, relying on thermal annealing[13,14] or by adding organic cosolvents,[15,16] acid solutions,[17,18] or ionic liquids (ILs).[19–21] Particularly, imidazolium-based ILs have proved to be excellent electrical conductivity enhancers, while at the same time acting as plasticizers to endow flexible PEDOT:PSS materials.[22,23] For instance, an outstanding enhancement of conductivity (from 0.4 to 2103 S/cm) was reported for PEDOT:PSS treated with 1-ethyl-3-methylimidazolium tetracyanoborate ([C_2MIM][B(CN)$_4$]) IL.[24] The fundamental behind this extraordinary conductivity increment is an ion exchange between PEDOT:PSS and the IL, helping PEDOT decouple from PSS and grow into large-scale conducting domains.[25,26] In another recent work, a stretchable and highly conductive (>1000 S/cm) electroluminescent device was developed from PEDOT:PSS/[C_2MIM][B(CN)$_4$] mixtures.[27]

Interestingly, the increase in the ionic strength by adding an IL can cause PEDOT:PSS dispersion to change into a solid-like gel, resulting from π–π stacking interactions of PEDOT.[28,29] Taking advantage of this phenomenon, Feig *et al*. prepared hydrogels of PEDOT:PSS and a secondary polymer network with the ionic liquid 4-(3-butyl-1-imidazolio)-1-butanesulfonic acid triflate, obtaining electrical conducitivities up to 23 S/cm and stretchable properties.[30] Moreover, Stringer *et al.* used microreactive inkjet printing to pattern different 2D and 3D structures of PEDOT:PSS/[C_2MIM][C_2SO_4] hydrogel, reaching electrical conductivities as high as 900 S/cm.[31]

Unfortunately, imidazolium-based ILs show acute toxicity and poor biodegradability,[32,33] turning their application in bioelectronics, where electrodes are in intimate contact with the skin, prohibitive. Therefore, biocompatibility is a key-sought specification for cutaneous electrodes, and novel electrolytes need to be urgently investigated. Recently, a natural deep eutectic solvent based on choline chloride and citric acid has been proposed as a dopant of PEDOT:PSS.[34] In the same direction, cholinium carboxylate ILs are an attractive family of biocompatible and biodegradable electrolytes that have been proven to have low biological activity and non-potential skin irritation.[35–37] Cholinium carboxylate ILs have already demonstrated an arresting performance in iongels for long-term cutaneous electrophysiology,[38–40] but the worth of these ILs as conductivity enhancers for PEDOT:PSS is still a matter of research.

In this work, a series of cholinium carboxylate ILs, including cholinium acetate ([Ch][Ac]), cholinium lactate ([Ch][Lac]), cholinium glycolate ([Ch][Glyco]), and cholinium glycerate ([Ch][Glyce]) are proposed as dopants of PEDOT:PSS to manufacture suitable electrodes for electrocardiogram (ECG) recordings. We focused on the impact of the anion on the conducting properties, thermal stability, and morphological changes in the polymer film structure. Furthermore, the behavior of some promising systems as injectable solid-like gels is also discussed.

Experimental

Materials

Poly(3,4-ethylenedioxythiophene): poly(styrene sulfonate) (PH1000, Heraeus Clevios™), choline bicarbonate ($C_5H_{14}NO{\cdot}HCO_3$, 80% in water, Sigma-Aldrich), acetic acid (CH_3CO_2H, ≥99.7%, Sigma-Aldrich), DL-lactic acid ($CH_3CH(OH)COOH$, ≈90%, Sigma-Aldrich), glycolic acid (ReagentPlus®, 99% Sigma-Aldrich), glyceric acid (Sigma-Aldrich), and p-toluenesulfonic acid monohydrate (ReagentPlus®, ≥98%, Sigma-Aldrich) were used as received.

Synthesis of cholinium-based ionic liquids

The cholinium carboxylate ILs used in this work, named cholinium acetate ([Ch][Ac]), cholinium lactate ([Ch][Lac]), cholinium glycolate ([Ch][Glyco]), cholinium glycerate ([Ch][Glyce]) and cholinium tosylate ([Ch][Tos]), were prepared by dropwise addition of the corresponding acid (1:1) to aqueous cholinium bicarbonate, as previously reported.[41] The mixtures were stirred at room temperature for 12 h. The resulting products were then washed three times with diethyl ether to remove the unreacted acid. Finally, the excess water and traces of diethyl ether were removed by rotary evaporation. The chemical structures and purities of the ILs were confirmed by ^{1}H-NMR, whose spectra can be found in Supporting Information (SI). The synthesized cholinium carboxylate ILs were dried prior to their use by stir-heating under vacuum at moderate temperature (≈45 °C, > 48 h).

Preparation of PEDOT:PSS/IL composites

PEDOT:PSS/cholinium-based IL composites were prepared by adding the desired ILs to PEDOT:PSS dispersion and subsequent mixing. Then, the prepared solutions were drop-casted and dried at 60°C under vacuum to obtain the corresponding films and membranes. Composites with PEDOT:PSS/ILs weight ratios of 90/10, 80/20, 70/30, 60/40, 50/50, and 40/60 were prepared with each ILs. The weight ratio was calculated without considering the water of PEDOT:PSS dispersion, thus, the established weight ratios are the final mass ratio between PEDOT:PSS and IL mass in the dried composite.[42] In addition, a physical gel was obtained by mixing PEDOT:PSS and [Ch][Lac] at a weight ratio of 60/40 and allowing the sample to equilibrate at room temperature until gelation occurred.

Characterization of composites

The electronic conductivity of the composite films was measured with an Ossila Four-Point Probe at room temperature.

The ionic conductivity of the composites was measured by electrochemical impedance spectroscopy using a VMP-3 potentiostat (Biologic Science Instruments). The samples were assembled in coin cells under an argon atmosphere between two stainless steel spacers. Each composite was studied in a heating and cooling ramp from 25 to 90°C in a frequency range of 1 MHz to 100 mHz using a voltage amplitude of 10 mV. The reported values are the average between the heating and cooling measurements. The samples were equilibrated for 30 min before each measurement.

The thermal stability of the composites was investigated using thermogravimetric analysis (TGA) performed on a TGA Q500 from TA Instruments. The measurements were carried out by heating the samples at 10 °C/min under a nitrogen atmosphere from 40 to 800 °C. The maximum decomposition temperature (Td_{max}) was determined as the main peak of the derivative weight loss curve.

Fourier transform infrared (FTIR) spectra of the materials were recorded on a Bruker Alpha II spectrophotometer employing a Platinum ATR module with a diamond window.

Atomic force microscope (AFM, Dimension ICON) was operated in the tapping mode using a TESP-V2 type silicon tips with a frequency of 320 kHz, a spring constant of 40 N/m, and a tip radius of 7nm. The commercially available PEDOT:PSS was spin coated as received, while the composites were dispersed in water at 1 mg/ml.

The rheological characterization was carried out with an AR-G2 rheomether (TA instruments) using a parallel plate geometry of 20 mm diameter and a gap of 300 µm. Time sweeps were performed at 1 Hz frequency and 1% strain for 2 hours. Frequency sweeps were performed from 0.01 to 10 Hz at 1% strain, and strain sweeps from 0.01 to 1000% were carried out at 1 Hz. The self-healing and injectability properties of the gels were tested by alternative strain changes of 1 and 1000%, for 180 seconds each, at 1 Hz. The experiments were performed at 25 °C.

Preparation of electrodes

Silver nanoparticle ink (Sicrys 130EG-1) was patterned using inkjet printing on a 50 µm thick polyimide (Kapton) substrate chosen due to its high flexibility to conform to simple human skin shapes. Electric

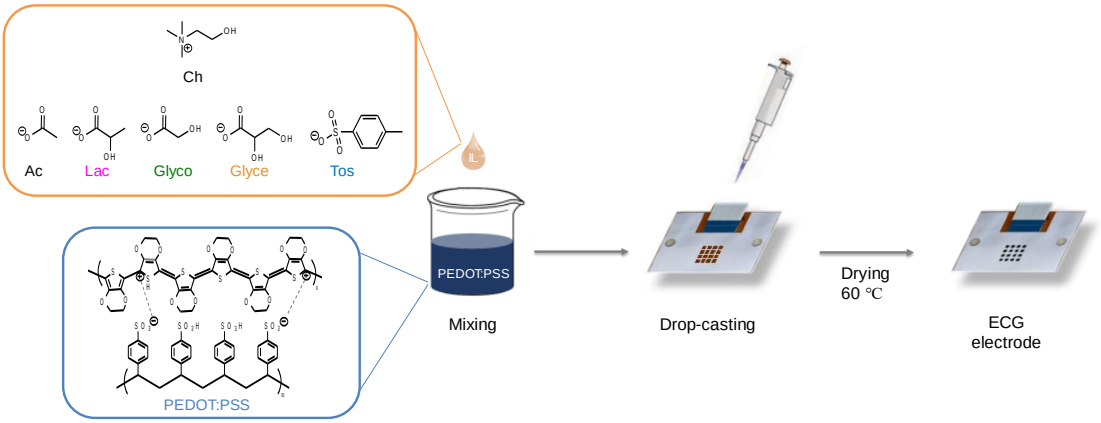

Figure 1 Chemical structures of PEDOT:PSS and ILs used and the general pathway for the preparation of PEDOT:PSS/IL composite electrodes.

tracks are insulated using a double-sided medical tape laser cut (VLS 2.30, Universal Laser Systems) to expose the electrodes' active area (1.5 by 1.5 mm^2). The bottom line was peeled off from the double-sided medical graded tape and aligned with Kapton using matching cut patterns in both layers and an auxiliary holder to ensure proper positioning. This process leaves a matrix of wells that were used for precise PEDOT:PSS/IL deposition and insulates the electric tracks between the electrodes and the contacts. A mixture of PEDOT:PSS, [Ch][Lac], and (glycidyloxypropyl)trimethoxysilane (GOPS, 1 wt%) was drop-casted into the wells and left to dry overnight at room temperature. The device is subsequently baked to evaporate solvents and crosslink PEDOT:PSS mixture prior to immersion in deionized (DI) water. A flat cable was attached using an anisotropic conducting film to achieve connection to external electronics. The fabrication was conducted as reported in Velasco-Bosom *et al.*[6]

Results and discussion

PEDOT:PSS/IL composites were prepared by combining PEDOT:PSS with various cholinium carboxylate ILs, which chemical structures are illustrated in Figure 1. The PEDOT:PSS/IL dispersions were drop-casted and dried at a mild temperature, obtaining flexible, self-standing, and blue-colored films.

A series of PEDOT:PSS/IL with weight ratios of 90/10, 80/20, 70/30, 60/40, 50/50, and 40/50 were prepared for the four cholinium carboxylate ILs, obtaining 24 different compositions of mixed conducting composites. In addition, [Ch][Tos] IL was included in this study for comparison purposes, since tosylate anion has been reported to be an excellent dopant of PEDOT,[42,43] although its biocompatibility could be questioned.

Figure 2 shows the electrical conductivity of the different composite formulations evaluated. It is believed that ion exchange between PEDOT:PSS and IL components helps PEDOT to decouple from PSS and to grow into large-scale conducting

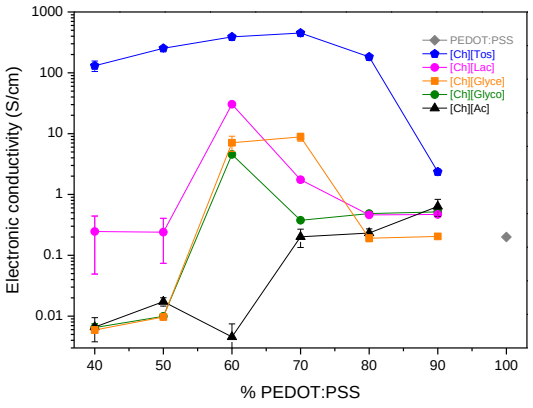

Figure 2 Electronic conductivities of PEDOT:PSS/IL composites at different PEDOT:PSS concentrations.

domains, but the exact mechanism is still under debate.[44] As expected, [Ch][Tos] displayed the highest conductivity enhancement for all the range of compositions studied, owing to the affinity of the tosylate anion with PEDOT, as it has the same sulfonate group as PSS.[42] Notably, by adding 30 wt% of this IL to PEDOT:PSS an electronic conductivity of 450 S/cm was obtained, compared with ≈0.2 S/cm for the untreated dispersion. As for the series of cholinium carboxylate ILs, the best electronic conductivity values followed the order: [Ch][Lac] (40 wt%) > [Ch][Glyce] (30 wt%) > [Ch][Glyco] (40 wt%) > [Ch][Ac] (10 wt%). Although the cholinium carboxylate ILs have similar chemical structures, it can be observed that acetate anion, without hydroxyl groups is the worse dopant in terms or electrical conductivity, which suggests the polarity of IL is important to have higher affinity with PEDOT and consequently, increased electrical conductivity. As can be seen, formulations containing between 30 and 40 wt% of ILs seem to be particularly suitable for boosting the PEDOT:PSS conductivity. Therefore, we used these compositions to further investigate the ionic conductivity *vs.* temperature dependence of the most promising systems (Figure 3).

Once again, [Ch][Tos] outperformed the ionic conductivity of the other cholinium carboxylate ILs in the whole temperature range analyzed for both 30 and 40 wt% IL compositions, as shown in Figures 3a and b. When comparing the ionic conductivities of composites with the same IL but having 30% or 40 wt% IL, we can observed that the conductivities are in the same range for [Ch[[Tos] and [Ch][Lac] at the two concentrations, however, ionic conductivity increases in one order of magnitude when increasing the amount of [Ch][Glyce] and [Ch][Glyco] from 30% to 40%. This is probably related to the compatibility of the IL with PEDOT:PSS and its ability of solvation. Between the cholinium carboxylate ILs, superior ionic conductivity profile was observed with [Ch][Lac] IL in both compositions (3×10^{-6} S/cm at room temperature for PEDOT:PSS/[Ch][Lac] (60/40) formulation, Figure 3b), due to a good compatibility of this IIL with PEDOT:PSS, forming a highly interconnected network facilitating the diffusion of the ions.

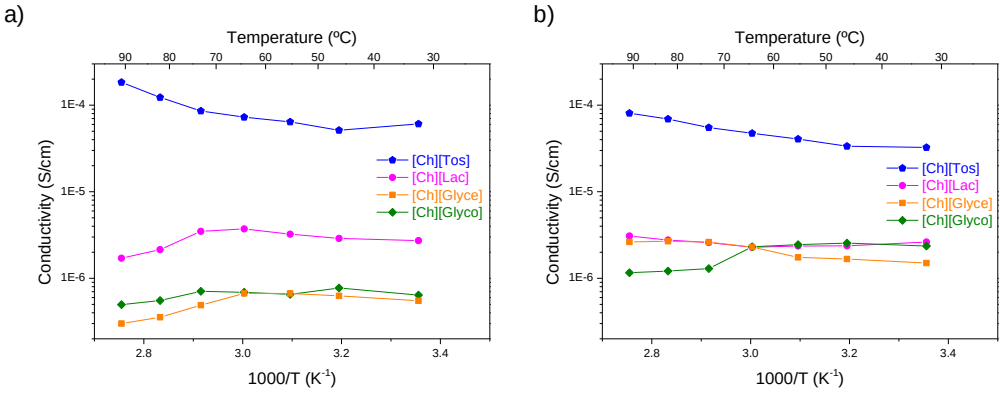

Figure 3 Ionic conductivities of PEDOT:PSS/IL composites at a) 70/30 and b) 60/40 compositions.

Then, we analyzed the thermal stability of the as-prepared PEDOT:PSS/IL 60/40 composite films. As shown in Figures 4a and S2 of the SI, the mixed conducting films were highly stable, with temperatures at 5% of weight loss ranging from 185-250 °C. Curiously, [Ch][Tos] showed a considerably lower decomposition temperature at 50% of weight loss (365 °C) compared with the other cholinium carboxylate ILs, which was around 600 °C. Among the ILs studied, [Ch][Lac] afforded the most thermally stable composite suggesting excellent compatibility with PEDOT:PSS. Indeed, FTIR analysis revealed that the characteristic vibrational modes of PEDOT:PSS (dashed gray lines in Figure 4b) at 1524 cm^{-1} (C=C ν), 1298 cm^{-1} (C-C skeletal vibrations), 950 cm^{-1} (S-O ν), 640 cm^{-1} (C-S ν), 1181 cm^{-1} (C-O-C ν), and 1062 cm^{-1} (C-O ν) red-shifted after adding [Ch][Lac] IL, confirming strong intermolecular interactions between both components. Meanwhile, the main peaks of [Ch][Lac] IL (dashed cyan lines) were located at 3150 cm^{-1} (O-H ν), 3027-2862 cm^{-1} (C-H ν, multiplet), 1590 cm^{-1} ($(COO)^-$ ν as), 1480 cm^{-1} ($(COO)^-$ ν sy), and 1120 cm^{-1} (C-N ν). Interestingly, the $(COO)^-$ signals of [Ch][Lac] IL are not present anymore in the PEDOT:PSS/ IL composite, indicating that lactate anion is effectively coupled to PEDOT displacing PSS.

If this ion exchange occurs, then phase segregation of the conducting polymer is expected. Therefore, we investigated the morphology of the PEDOT:PSS/ILs composite films by AFM to gain more insights into this phenomenon. Figure 4c shows the AFM phase images obtained for neat PEDOT:PSS, PEDOT:PSS/[Ch][Lac] (60/40), and PEDOT:PSS/[Ch][Tos] (60/40) composites. The neat PEDOT:PSS displayed a globular nanostructure, probably consisting of homogeneously mixed PEDOT-core and PSS-shell grains, which is in agreement to what

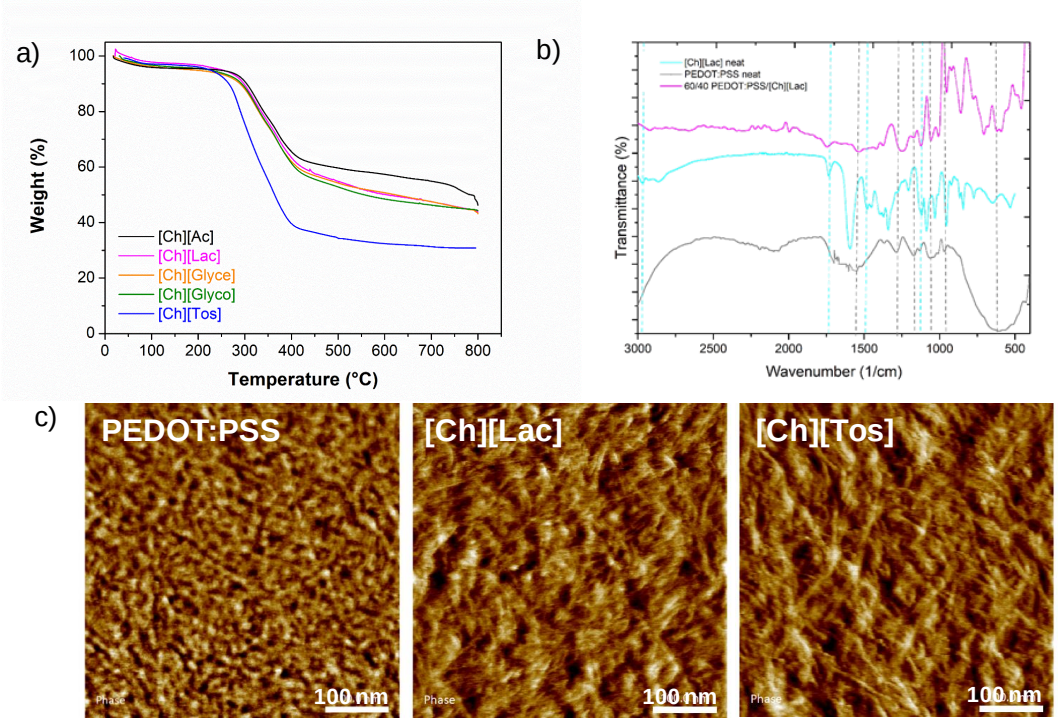

Figure 4 a) TGA curves of PEDOT:PSS/IL composites at 60/40 compositions; b) FTIR analysis of pure PEDOT:PSS, pure [Ch][Lac] and their composite at 60/40 composition; c) AFM phase images of pure PEDOT:PSS, PEDOT:PSS/[Ch][Lac] 60/40 and PEDOT:PSS/[Ch][Tos] 60/40 composite films.

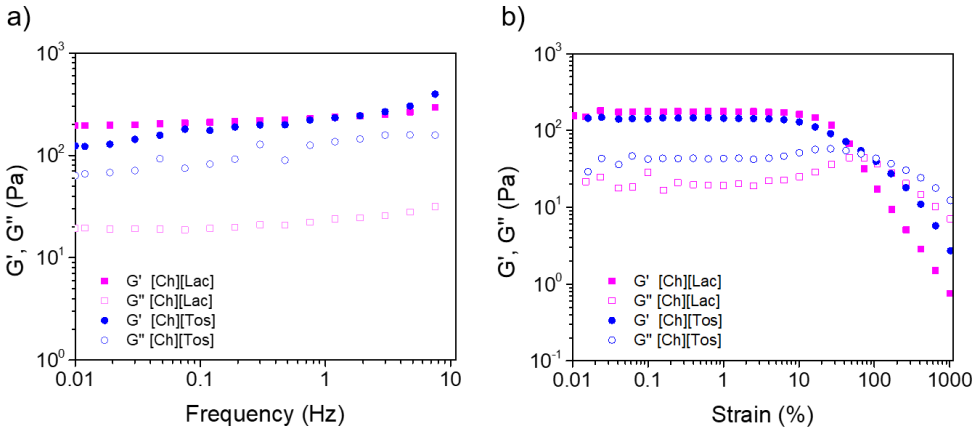

Figure 5 Storage modulus (G') and loss modulus (G'') of PEDOT:PSS with 40% of [Ch][Lac] or [Ch][Tos] as a function of a) frequency; and b) strain.

has been previously reported.[34] After adding [Ch][Lac] IL, these globular grains grew into large-scale domains, confirming the PEDOT phase separation. The incorporation of [Ch][Tos] IL led to similar surface morphology. These large interconnected regions of PEDOT correlate well with the increase in the electrical conductivity from 0.2 S/cm to ≈30 and 450 S/cm for the composites containing the [Ch][Lac] and [Ch][Tos] ILs, respectively.

Since the good mixed ionic and electronic conductivity of PEDOT:PSS composites containing 40 wt% of [Ch][Tos] and [Ch][Lac] ILs, we investigated the rheological behavior of these formulations. The evolution of the elastic (G') and loss (G'') moduli over time after mixing 60 wt% of PEDOT:PSS with 40 wt% of [Ch][Tos] or [Ch][Lac] ILs was firstly studied (Figure S8). The addition of [Ch][Lac] IL lead to an instantaneous gelation, with values of G' higher than G'' from the starting point. In the case of the addition of [Ch][Tos] IL, the G'' was higher than G' up to 1500 s when a crossover point of the dynamic moduli was observed (G'>G''), which indicated the gelation point of PEDOT:PSS/[Ch][Tos] gel. The lower kinetics of gelation with [Ch][Tos] IL can be related to the solid nature of the material, that needs to be first dissolved, in order to form the gel by ionic interactions with PEDOT:PSS. Then, the viscoelastic properties of the gels at the steady state were investigated to determine the storage modulus G' and the loss modulus G'' (Figure 5a). Both gels showed elastic moduli (G') in the order of 10^2 Pa and the frequency sweeps revealed that are stable in the frequency range of 0.01-10 Hz. When keeping the frequency fixed and varying the strain (Figure 5b), the gels presented a linear viscoelastic regime with constant values of G' and G'' up to 10% strain, and a gel behavior up to 60% strain, when the gels are disrupted and became liquid, which can be interesting for the processing of these materials.

Moreover, due to the dynamic nature of the physically crosslinked gels, we further explored their injectability properties by alternating amplitude oscillatory shear. The results obtained for PEDOT:PSS with 40 wt% of [Ch][Lac] and [Ch][Tos] ILs are shown in Figure 6. It is observed that at 1% strain, both materials are featured by a stable solid-like behavior (G'> G'') as shown previously. When a significant amplitude strain is applied (1000%), G' instantaneously dropped and became lower than G'', indicating the collapse of the network and becoming liquid like. When the applied strain was returned to 1%, the materials fully recovered its initial moduli values without delay, unveiling a rapid self-healing ability and a reversible gel-sol transition. This viscoelastic behavior is a key-sought specification for injectable materials and uncovers the

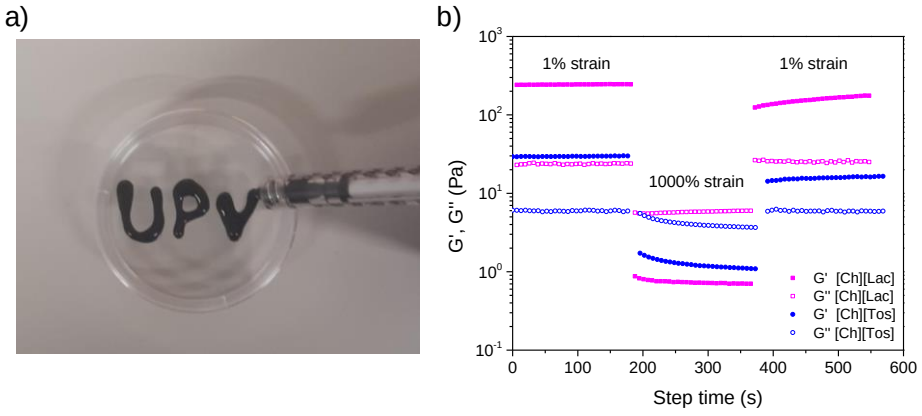

Figure 6 a) Injectability test of PEDOT:PSS/[Ch][Lac] 60/40 composition with 1 mL syringe; and b) G' and G'' of PEDOT:PSS/[Ch][Lac] 60/40 and PEDOT:PSS/[Ch][Tos] 60/40 gels under a continuous strain sweep with alternating oscillation forces at 1% and 1000% of strain.

potentiality of these gels for 3D printing applications by mild extrusion.

Finally, as a promising composite material benefiting from potential biocompatibility and high mixed conductivity, PEDOT:PSS/[Ch][Lac] 60/40 was used to manufacture flexible electrodes for ECG recording. The material was dropcasted on the silver contacts of an inkjet printed multielectrode array to reduce interfacial impedance with skin.[6] Typical ECG recordings of PEDOT:PSS/[Ch][Lac] (60/40) electrode is shown in Figure 7. For comparison, an ECG signal using a commercial electrode (DENIS10026, Spes Medica) has been recorded using an equivalent setup. It is possible to observe that signal amplitudes and noise levels are comparable in both cases. The characteristic waveform of the heart activity (PQRST), essential to establish cardiovascular disease diagnostics, is clearly recorded by both electrodes with high reproducibility. Furthermore, a remarkably stable signal baseline with low noise is observed, stemming from the excellent combined ionic and electronic conductivity of this composite electrode (≈3×10^{-6} and 30 S/cm, respectively). The capacity to record high-quality ECG signals makes these electrodes great candidates for fabricating long-lasting wearable electronics.

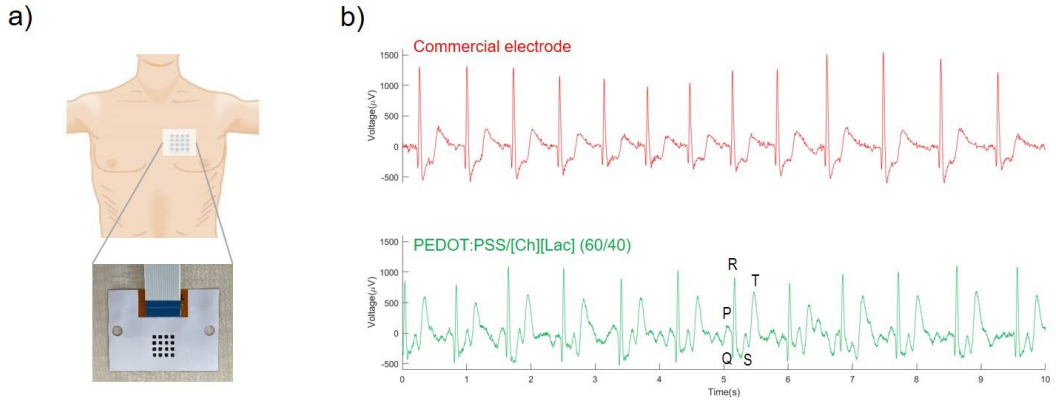

Figure 7 a) Schematic presentation of the electrodes that were placed on the chest of a male volunteer. b) ECG signals recording of heart activity during an electrocardiography experiment: Top signal recorded with commercial electrode; bottom signal recorded with PEDOT:PSS/[Ch][Lac] (60/40) electrode.

Conclusions

In this article, we present for the first time the use of biocompatible ILs, derived from cholinium cation and carboxylate anions, as dopants of PEDOT:PSS conducting polymer. Among the different ILs evaluated, [Ch][Tos] and [Ch][Lac] ILs seem to have the highest affinity for PEDOT:PSS, leading to an enhancement in the electronic conductivity of three and two orders of magnitude, respectively. This improvement on the conducting properties is directly linked to the decoupling of PEDOT from PSS, followed by PEDOT phase segregation into large conducting domains, as demonstrated by AFM analysis. Moreover, rheological measurements revealed that PEDOT:PSS underwent fast gelation (15-50 min) only at defined ILs contents. Interestingly, the obtained gels showed rapid recovery upon large strains, disclosing the attractiveness of these soft materials for 3D printing applications. Ultimately, with inherent biocompatibility and good conducting performance, PEDOT:PSS/[Ch][Lac] composite proved to be efficient for high-quality ECG recording, obtaining smooth signals with negligible noise.

Altogether, the obtained results demonstrated that cholinium carboxylate ILs could expand the prospect of PEDOT: PSS toward bioelectronics applications, where harmful conductivity-enhancer additives can cause tissue damage. Finally, this work also encourages researchers to find new biocompatible alternatives to cholinium carboxylate ILs as dopants of semiconducting polymers.

Conflicts of interest

There are no conflicts to declare.

Acknowledgements

This work was supported by Marie Sklodowska-Curie Research and Innovation Staff Exchanges (RISE) under the grant agreement No 823989 "IONBIKE" and AEI-MINECO for project PID2020-119026GB-I00. The financial support received from CONICET and ANPCyT (Argentina) is also gratefully acknowledged. Nerea Casado would like to thank the University of the Basque Country (No. 823989) for funding through a specialization of research staff fellowship (ESPDOC 19/99). Santiago Velasco-Bosom acknowledges the support from W.D Armstrong Studentship. Liliana C. Tomé is grateful to FCT (Fundação para a Ciência e a Tecnologia) in Portugal for her research contract under Scientific Employment Stimulus (2020.01555.CEECIND). Associate Laboratory for Green Chemistry – LAQV also acknowledges the financial support from FCT/MCTES (UIDB/50006/2020 and UIDP/50006/2020).

References

1 T. Cheng, F. Wang, Y.-Z. Zhang, L. Li, S.-Y. Gao, X.-L. Yang, S. Wang, P.-F. Chen and W.-Y. Lai, *Chemical Engineering Journal*, 2022, **450**, 138311.

2 T. Cheng, L. Li, Y. Chen, S. Yang, X. Yang, Z. Liu, J. Qu, C. Meng, Y. Zhang and W. Lai, *Adv Mater Interfaces*, 2022, 2201137.

3 S. Zhang, Y. Chen, H. Liu, Z. Wang, H. Ling, C. Wang, J. Ni, B. Çelebi-Saltik, X. Wang, X. Meng, H. Kim, A. Baidya, S. Ahadian, N. Ashammakhi, M. R. Dokmeci, J. Travas-Sejdic and A. Khademhosseini, *Advanced Materials*, 2020, **32**, 1904752.

4 G. C. Luque, M. L. Picchio, A. P. S. Martins, A. Dominguez-Alfaro, N. Ramos, I. del Agua, B. Marchiori, D. Mecerreyes, R. J. Minari and L. C. Tomé, *Adv Electron Mater*, , DOI:10.1002/aelm.202100178.

5 H. Yin, Y. Zhu, K. Youssef, Z. Yu and Q. Pei, *Advanced Materials*, 2021.

6 S. Velasco-Bosom, N. Karam, A. Carnicer-Lombarte, J. Gurke, N. Casado, L. C. Tomé, D. Mecerreyes and G. G. Malliaras, *Adv Healthc Mater*, , DOI:10.1002/adhm.202100374.

7 M. Papaiordanidou, S. Takamatsu, S. Rezaei-Mazinani, T. Lonjaret, A. Martin and E. Ismailova, *Adv Healthc Mater*, , DOI:10.1002/adhm.201600299.

8 I. del Agua, D. Mantione, U. Ismailov, A. Sanchez-Sanchez, N. Aramburu, G. G. Malliaras, D. Mecerreyes and E. Ismailova, *Adv Mater Technol*, 2018, **3**, 1–8.

9 E. Bihar, T. Roberts, E. Ismailova, M. Saadaoui, M. Isik, A. Sanchez-Sanchez, D. Mecerreyes, T. Hervé, J. B. De Graaf and G. G. Malliaras, *Adv Mater Technol*, 2017, **2**, 2–6.

10 U. Kraft, F. Molina-Lopez, D. Son, Z. Bao and B. Murmann, *Adv Electron Mater*, 2020, **6**, 1900681.

11 Y. Xia and J. Ouyang, *ACS Appl Mater Interfaces*, , DOI:10.1021/am300881m.

12 A. De Izarra, S. Park, J. Lee, Y. Lansac and Y. H. Jang, *J Am Chem Soc*, , DOI:10.1021/jacs.7b10306.

13 B. Friedel, P. E. Keivanidis, T. J. K. Brenner, A. Abrusci, C. R. McNeill, R. H. Friend and N. C. Greenham, *Macromolecules*, , DOI:10.1021/ma901182u.

14 X. Huang, L. Deng, F. Liu, Q. Zhang and G. Chen, *Energy Material Advances*, , DOI:10.34133/2021/1572537.

15 J. P. Thomas, L. Zhao, D. McGillivray and K. T. Leung, *J Mater Chem A Mater*, , DOI:10.1039/c3ta14590e.

16 Q. Wei, M. Mukaida, Y. Naitoh and T. Ishida, *Advanced Materials*, , DOI:10.1002/adma.201205158.

17 Z. Fan, P. Li, D. Du and J. Ouyang, *Adv Energy Mater*, , DOI:10.1002/aenm.201602116.

18 J. Ouyang, *ACS Appl Mater Interfaces*, , DOI:10.1021/am404113n.

19 M. Döbbelin, R. Marcilla, C. Pozo-Gonzalo and D. Mecerreyes, *J Mater Chem*, , DOI:10.1039/c0jm00114g.

20 C. Choi, A. De Izarra, I. Han, W. Jeon, Y. Lansac and Y. H. Jang, *Journal of Physical Chemistry B*, , DOI:10.1021/acs.jpcb.1c09001.

21 Y. Wang, C. Zhu, R. Pfattner, H. Yan, L. Jin, S. Chen, F. Molina-Lopez, F. Lissel, J. Liu, N. I. Rabiah, Z. Chen, J. W. Chung, C. Linder, M. F. Toney, B. Murmann and Z. Bao, *Sci Adv*, , DOI:10.1126/sciadv.1602076.

22 M. Döbbelin, R. Marcilla, M. Salsamendi, C. Pozo-Gonzalo, P. M. Carrasco, J. A. Pomposo and D. Mecerreyes, *Chemistry of Materials*, , DOI:10.1021/cm070398z.

23 N. Saxena, B. Pretzl, X. Lamprecht, L. Bießmann, D. Yang, N. Li, C. Bilko, S. Bernstorff and P. Müller-Buschbaum, *ACS Appl Mater Interfaces*, , DOI:10.1021/acsami.8b21709.

24 S. Kee, N. Kim, B. S. Kim, S. Park, Y. H. Jang, S. H. Lee, J. Kim, J. Kim, S. Kwon and K. Lee, *Advanced Materials*, , DOI:10.1002/adma.201505473.

25 N. A. Shahrim, Z. Ahmad, A. Wong Azman, Y. Fachmi Buys and N. Sarifuddin, *Mater Adv*, 2021.

26 C. M. Palumbiny, F. Liu, T. P. Russell, A. Hexemer, C. Wang and P. Müller-Buschbaum, *Advanced Materials*, , DOI:10.1002/adma.201500315.

27 M. Y. Teo, N. Kim, S. Kee, B. S. Kim, G. Kim, S. Hong, S. Jung and K. Lee, *ACS Appl Mater Interfaces*, , DOI:10.1021/acsami.6b11988.

28 M. A. Leaf and M. Muthukumar, *Macromolecules*, , DOI:10.1021/acs.macromol.6b00740.

29 V. R. Feig, H. Tran, M. Lee and Z. Bao, *Nat Commun*, , DOI:10.1038/s41467-018-05222-4.

30 V. R. Feig, H. Tran, M. Lee and Z. Bao, *Nat Commun*, 2018, **9**, 2740.

31 M. Y. Teo, N. Ravichandran, N. Kim, S. Kee, L. Stuart, K. C. Aw and J. Stringer, *ACS Appl Mater Interfaces*, , DOI:10.1021/acsami.9b12069.

32 A. Romero, A. Santos, J. Tojo and A. Rodríguez, *J Hazard Mater*, , DOI:10.1016/j.jhazmat.2007.10.079.

33 I. F. Mena, E. Diaz, J. Palomar, J. J. Rodriguez and A. F. Mohedano, *Chemosphere*, , DOI:10.1016/j.chemosphere.2019.124947.

34 Y. Lu, R. Liu, X. C. Hang and D. J. Young, *Polym Chem*, , DOI:10.1039/d1py00064k.

35 M. Petkovic, J. L. Ferguson, H. Q. N. Gunaratne, R. Ferreira, M. C. Leitão, K. R. Seddon, L. P. N. Rebelo and C. S. Pereira, *Green Chemistry*, 2010, **12**, 643–64.

36 J. M. Gomes, S. S. Silva and R. L. Reis, *Chem Soc Rev*, 2019.

37 R. Vijayaraghavan, B. C. Thompson, D. R. MacFarlane, R. Kumar, M. Surianarayanan, S. Aishwarya and P. K. Sehgal, *Chemical Communications*, , DOI:10.1039/b910601d.

38 M. Isik, T. Lonjaret, H. Sardon, R. Marcilla, T. Herve, G. G. Malliaras, E. Ismailova and D. Mecerreyes, *J Mater Chem C Mater*, 2015, **3**, 8942–8948.

39 A. Aguzin, G. C. Luque, L. I. Ronco, I. del Agua, G. Guzmán-González, B. Marchiori, A. Gugliotta, L. C. Tomé, L. M. Gugliotta, D. Mecerreyes and R. J. Minari, *ACS Biomater Sci Eng*, 2022, **8**, 2598–2609.

40 G. C. Luque, M. L. Picchio, A. P. S. Martins, A. Dominguez-Alfaro, N. Ramos, I. del Agua, B. Marchiori, D. Mecerreyes, R. J. Minari and L. C. Tomé, *Adv Electron Mater*, 2021, **7**, 2100178.

41 T. Mourão, L. C. Tomé, C. Florindo, L. P. N. Rebelo and I. M. Marrucho, *ACS Sustain Chem Eng*, , DOI:10.1021/sc500444w.

42 D. R. Evans, *Chemical Communications*, 2022, **58**, 4553–4560.

43 N. Delavari, J. Gladisch, I. Petsagkourakis, X. Liu, M. Modarresi, M. Fahlman, E. Stavrinidou, M. Linares and I. Zozoulenko, *Macromolecules*, , DOI:10.1021/acs.macromol.1c00723.

44 H. Shi, C. Liu, Q. Jiang and J. Xu, *Adv Electron Mater*, 2015, **1**, 1500017.